

## Landau–Zener transitions in qubits controlled by electromagnetic fields

Martijn Wubs<sup>1,4</sup>, Keiji Saito<sup>2</sup>, Sigmund Kohler<sup>1</sup>,  
Yosuke Kayanuma<sup>3</sup> and Peter Hänggi<sup>1</sup>

<sup>1</sup> Institut für Physik, Universität Augsburg, Universitätsstraße 1,  
D-86135 Augsburg, Germany

<sup>2</sup> Department of Physics, Graduate School of Science, University of Tokyo,  
Bunkyo-Ku, Tokyo 113-0033, Japan

<sup>3</sup> Department of Mathematical Science, Graduate School of Engineering,  
Osaka Prefecture University, Sakai 599-8531, Japan

E-mail: [Martijn.Wubs@Physik.Uni-Augsburg.de](mailto:Martijn.Wubs@Physik.Uni-Augsburg.de)

*New Journal of Physics* 7 (2005) 218

Received 5 August 2005

Published 11 October 2005

Online at <http://www.njp.org/>

doi:10.1088/1367-2630/7/1/218

**Abstract.** We investigate the influence of a dipole interaction with a classical radiation field on a qubit during a continuous change of a control parameter. In particular, we explore the non-adiabatic transitions that occur when the qubit is swept with linear speed through resonances with the time-dependent interaction. Two classic problems come together in this model: the Landau–Zener (LZ) and the Rabi problem. The probability of LZ transitions now depends sensitively on the amplitude, the frequency and the phase of the Rabi interaction. The influence of the static phase turns out to be particularly strong, since this parameter controls the time-reversal symmetry of the Hamiltonian. In the limits of large and small frequencies, analytical results obtained within a rotating-wave approximation compare favourably with a numerically exact solution. We discuss physical realizations in microwave optics, quantum dots and molecular nanomagnets.

<sup>4</sup> Author to whom any correspondence should be addressed.

**Contents**

<b>1. Introduction</b>	<b>2</b>
<b>2. The LZ model with harmonic interaction modulation</b>	<b>3</b>
<b>3. Adiabatic versus non-adiabatic transitions</b>	<b>5</b>
3.1. Adiabatic following . . . . .	5
3.2. Non-adiabatic regime . . . . .	6
<b>4. Exploring the crossover region</b>	<b>8</b>
<b>5. Phase dependence</b>	<b>9</b>
5.1. Transfer-matrix approach . . . . .	10
5.2. Time-reversal anti-symmetry . . . . .	10
<b>6. Discussion and summary</b>	<b>11</b>
<b>Acknowledgments</b>	<b>13</b>
<b>References</b>	<b>13</b>

**1. Introduction**

An essential ingredient to a quantum computer is a set of parameters that is controllable in the sense that it is possible to manipulate the parameter values at any time such that the qubits undergo one-qubit or two-qubit gate operations. For quantum computer implementations that rely on nuclear magnetic resonance [1] or on spins in quantum dots [2], such a manipulation is possible by switching magnetic fields that act on the qubit. This includes the possibility of inverting the sign of the field. Thereby, the diabatic energy levels of the qubit typically cross. If at the same time a second magnetic field acts in any other direction, the adiabatic levels form an *avoided* crossing instead of an exact crossing. Then, depending on the speed at which the control parameters are manipulated, the state of the qubit can follow the adiabatic energy levels or undergoes a non-adiabatic, so-called Landau–Zener (LZ) transition to the opposite branch ([3]–[5], [7] see also [6].<sup>5</sup>)

In the context of quantum computation, it has been proposed to exploit LZ transitions for improving the readout of qubits via the so-called Zener flip quantum tunnelling [8]. This mechanism has recently been implemented for flux qubits [9]. A method for non-adiabatic electron manipulation in quantum dots also relies on LZ transitions [10]. Moreover, the observation of LZ transitions is a clear sign of coherence like, e.g., optical coherence in a classical optical-ring resonator [11] or macroscopic quantum coherence in superconducting loops [12, 13]. LZ transitions have also been used to determine tiny interactions between levels in molecular clusters [14, 15]. While in these cases, LZ transitions are beneficial, the opposite is true in the case of adiabatic quantum computing [16, 17]. There, the computation is performed by a quantum system that follows adiabatically the instantaneous ground state of a slowly varying Hamiltonian and, consequently, the emergence of any non-adiabatic transition constitutes an error source.

The physical origin of a coupling between two levels of a quantum system is not necessarily simply an overlap between the respective wave functions. In particular for spins and atoms, such a coupling typically stems from the dipole interaction of the system with a radiation field.

<sup>5</sup> This paper contains an exact solution of the LZ model based on a perturbation expansion including all orders.

In a seminal work [18] (see also [19]), Rabi predicted within an exact quantum mechanical treatment that a classical, monochromatic and circularly polarized radiation field induces spin rotations with a frequency which at resonance is proportional to the field amplitude. With resonant linearly polarized light, the same characteristic harmonic Rabi oscillations of atomic inversions are observed. As a consequence of the linearly polarized driving, the optical realization of the Rabi problem is not exactly solvable. For resonant excitations, however, it is possible to apply a rotating-wave approximation (RWA) which formally restores the situation with circular polarization [20, 21]. This necessarily neglects effects beyond RWA like the Bloch–Siegert shift of the resonance frequency. In optical realizations, however, such effects are very tiny [20, 22].

The question now arises whether a level interaction mediated by a classical monochromatic radiation field can induce LZ transitions in a two-level system as its energies cross. In this work, we demonstrate that this is indeed the case. Thereby, we investigate LZ transitions that are induced by the coupling of a spin to a linearly polarized light field, henceforth referred to as Rabi coupling. In the traditional LZ problem, non-adiabatic transitions occur when the adiabatic energy levels are close to each other. By contrast, we will find that with a Rabi coupling to a high-frequency field, the transitions take place at times at which the radiation field is at resonance with the diabatic energy levels. This allows for sufficiently weak coupling a perturbative treatment within a RWA. For suitably chosen parameters, the driving reduces the probability for LZ transitions which relates this problem to the so-called coherent destruction of tunnelling [23]–[25].

A different kind of time-dependence would be provided by coupling the two-level system to a noise source. In this paper, we will work in the limit relevant for quantum computation instead, namely the coherent limit. In relation to this, it is interesting to note that LZ tunnelling is fairly robust against classical noise [6], [26]–[28] and quantum dissipation [29]–[35]. In this context, we also like to emphasize that herein considered LZ tunnelling due to coupling to a light field is different from the one considered in [13, 36, 37] where it is the diabatic energies of the two-level system that are subjected to a time-periodic modulation (the so-called dynamic Stark effect).

The model considered here applies quite generally to qubits that are driven by *two* external fields: firstly, the interaction between the two levels varies harmonically in time due to interaction with a transverse external field that causes a negligible dynamic Stark effect. Secondly, the qubit level spacing is controlled by an external field that varies linearly in time. Without driving, the interaction between the levels should be negligible. Possible realizations of such well-controlled two-level systems are of interest for quantum-information processing. Examples are not only the natural spin- $\frac{1}{2}$  systems in magnetic fields, but also effective two-level systems in nanostructures, such as coupled quantum dots, quantum wires, or quantum wells. These solid-state qubits have received heightened attention recently, since they can be well controlled and potentially be scaled up to larger quantum systems. Much work on such driven quantum systems deals with transport problems [7], [38]–[40]. In the discussion at the end of the paper, we detail some physical realizations of our scheme.

## 2. The LZ model with harmonic interaction modulation

We consider a quantum system (‘atom’) with two relevant energy levels  $|1\rangle$  and  $|2\rangle$  whose time-dependent energies  $\pm Vt/2$  cross at  $t = 0$ . Both levels are coupled by a classical dipole field with frequency  $\Omega$  and phase  $\phi$ . The effective amplitude  $g$  is given by field strength times the dipole

moment of the two-level system. Thus, the Hamiltonian reads

$$H(t) = \frac{Vt}{2}\sigma_z + f(t)\sigma_x, \quad f(t) = g \cos(\Omega t + \phi), \quad (1)$$

where  $\sigma_z|1\rangle = |1\rangle$  and  $\sigma_z|2\rangle = -|2\rangle$ . Moreover, we assume that at time  $t = -\infty$ , the system is in its instantaneous ground state, i.e.  $|\psi(-\infty)\rangle = |1\rangle$ . If the energies in the first term were time-independent, and if the field were in resonance with the atomic energy difference, then this Hamiltonian would describe an atom undergoing Rabi oscillations. If the field strength of the ac field vanished, then no transitions between the levels could occur, which means that the Hamiltonian (1) models a special type of ‘photon-assisted transport’ [38].

Since for most times, the Hamiltonian (1) is dominated by its first term, a proper interaction-picture representation is provided by the transformation  $U_0(t) = \exp(-iVt^2\sigma_z/2\hbar)$ , that is  $|\psi(t)\rangle = U_0(t)|\tilde{\psi}(t)\rangle$  and  $|\tilde{\psi}(t)\rangle = \tilde{c}_1(t)|1\rangle + \tilde{c}_2(t)|2\rangle$ , where the interaction-picture probability amplitudes obey

$$\begin{pmatrix} \dot{\tilde{c}}_1 \\ \dot{\tilde{c}}_2 \end{pmatrix} = -\frac{i}{\hbar} \begin{pmatrix} 0 & f(t) e^{iVt^2/2\hbar} \\ f(t) e^{-iVt^2/2\hbar} & 0 \end{pmatrix} \begin{pmatrix} \tilde{c}_1 \\ \tilde{c}_2 \end{pmatrix}. \quad (2)$$

For  $\Omega = \phi = 0$ , the Hamiltonian (1) defines the standard LZ problem for which the exact solution of the equation of motion (2) can be expressed in terms of parabolic cylinder functions [3]. Then, the time-evolution from  $t = -\infty$  to  $t = \infty$  is given by the S-matrix

$$\mathbf{S}_g = \begin{pmatrix} \sqrt{q} & \sqrt{1-q} e^{-i\chi} \\ -\sqrt{1-q} e^{i\chi} & \sqrt{q} \end{pmatrix}, \quad (3)$$

where  $q = \exp(-2\pi g^2/\hbar V)$  and the Stokes phase  $\chi = \pi/4 + \arg \Gamma(1 - i\delta) + \delta(\ln \delta - 1)$ , with  $\delta = g^2/(\hbar V)$  and  $\Gamma(\dots)$  the Gamma function. The famous LZ transition probability follows readily: the probability  $P$  that the atom ends up in the initially unoccupied level  $|2\rangle$  is

$$P \equiv |c_2(t = \infty)|^2 = 1 - e^{-2\pi g^2/\hbar V}. \quad (4)$$

Note that this result is exact for all values of  $g$  and  $V$ .

Already a good approximation to the time-dependent solution is provided by the fact that for  $f(t) = g$  and sufficiently large times, the phase factors in the matrix in equation (2) are rapidly oscillating with a quadratic time dependence. As a consequence,  $\tilde{c}_1$  and  $\tilde{c}_2$  remain essentially constant. By contrast, close to  $t = 0$ , these phase factors assume stationary values and the two-level system undergoes a transition. This means that S-matrix (3) in fact describes a transition taking place at  $t = 0$ . Thus, in the interaction picture the dynamics is approximately given by  $|\tilde{\psi}(t)\rangle = |\tilde{\psi}(-\infty)\rangle$  for  $t < 0$  and  $|\tilde{\psi}(t)\rangle = \mathbf{S}_g|\tilde{\psi}(\infty)\rangle$  for  $t > 0$ .

For  $\Omega \neq 0$ , the time  $t = 0$  no longer marks the time at which the phase is stationary and the behaviour changes significantly, as we will see below. In order to anticipate the richness of the resulting dynamics, we have numerically integrated the equations of motion (2) for  $\phi = 0$  and various coupling strengths  $g$  and frequencies  $\Omega$ . Figure 1 depicts the time dependence of the probability  $|c_2(t)|^2$  to find the atom in the initially unpopulated level  $|2\rangle$ .

For small interaction  $g$  (see lower five plots in figure 1), the final-transition probability for long times does not depend strongly on frequency, although the curves differ strongly around  $t = 0$ . The most interesting feature of figure 1 is that for high frequencies,  $\Omega \gg \sqrt{V/\hbar}$ , the dynamics consists of two (almost) independent transitions.

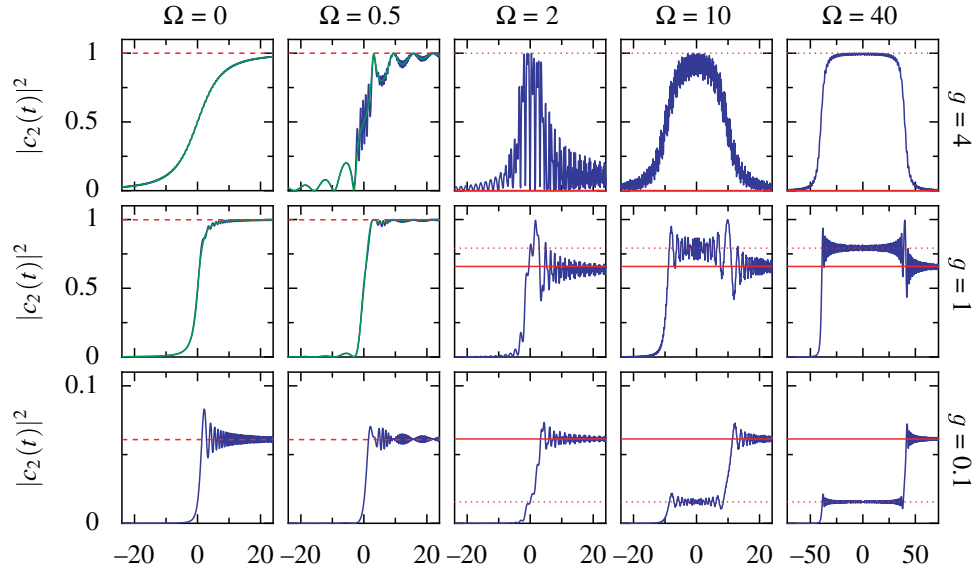


**Figure 1.** LZ transition probability  $|c_2(t)|^2$  as a function of time in units of  $(\hbar/V)^{1/2}$  for  $\phi = 0$  and various values of the interaction strength  $g$  in units  $(\hbar V)^{1/2}$  and the modulation frequency  $\Omega$  in units of  $(V/\hbar)^{1/2}$ . The red lines mark the standard LZ-transition probability (equation (4), dashed), the RWA result for a double transition (equation (9), solid), and the transition probability at the intermediate stage (equation (10), dotted). The green curves in the four upper-left panels correspond to the adiabatic-following result equation (5).

### 3. Adiabatic versus non-adiabatic transitions

In the standard LZ problem, one distinguishes two limiting cases: if the level crossing occurs very rapidly, the potential switches practically instantaneously such that no significant dynamics can take place. The system will then remain in level  $|1\rangle$ , so that finally  $P = 0$ . In the opposite limit the instantaneous energy levels change very slowly. The system then follows adiabatically the lower-energy level  $|E_-(t)\rangle$  and ends up with  $P = 1$ .

#### 3.1. Adiabatic following

Adiabatic following means that transitions between the instantaneous eigenstates can be neglected. The criterion for adiabatic following is that at each instance of time, the coupling between the adiabatic energies is ‘sufficiently small’, much smaller than the energy splitting. Stated in mathematical terms, this requirement becomes  $|\langle E_-(t) | \frac{d}{dt} | E_+(t) \rangle| \ll |E_+(t) - E_-(t)|/\hbar$ . This gives for the standard LZ problem a splitting  $2g$  and the adiabaticity condition  $\hbar V \ll g^2$ .

For the time-dependent two-state Hamiltonian (1), the condition for adiabatic following becomes more involved, because the minimal splitting of the adiabatic energies  $E_{\pm}(t) = \pm\sqrt{(Vt/2)^2 + f^2(t)}$  depends not only on the coupling strength  $g$  but also on the frequency  $\Omega$  and the phase  $\phi$ . The minimal splitting will never be larger than  $2g$ , whatever the frequency and phase. The sensitive dependence on the phase becomes obvious from figure 2: in particular

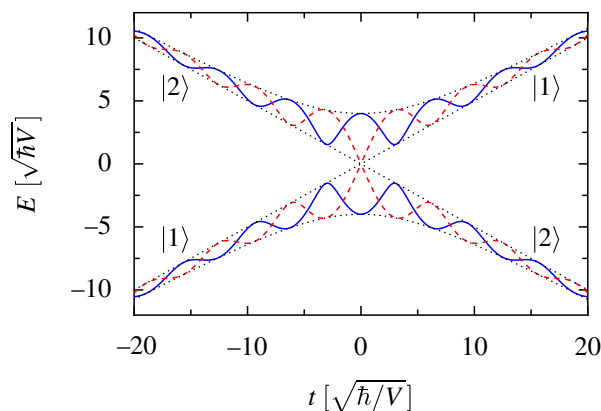


**Figure 2.** Adiabatic energies  $E_{\pm}(t)$  for a Rabi coupling with  $\phi = 0$  (solid lines) and  $\phi = \pi/2$  (dashed). The dotted lines marked the limiting values for  $g = 0$  and the standard LZ model with constant coupling, respectively. The other parameters are  $g = 4\sqrt{\hbar V}$  and  $\Omega = 0.5\sqrt{V/\hbar}$ .

for  $\phi = \pi/2$ , the adiabatic spectrum no longer exhibits an avoided crossing but rather an exact crossing, since at time  $t = 0$  both terms in the Hamiltonian (1) vanish simultaneously. Consequently, the adiabaticity condition is violated irrespective of the values of the  $g$  and  $\Omega$ . This qualitative difference already provides a hint that the phase  $\phi$  has a strong influence on the population dynamics.

By contrast, for a phase  $\phi \neq \pi/2 \pmod{\pi}$ , the energies  $E_{\pm}$  never form an exact crossing. Thus, it is always possible to choose  $V$  and  $\Omega$  so small that the adiabaticity condition is fulfilled. Then, by making the time-dependent transformation to the instantaneous-energy representation, neglecting there the off-diagonal elements in the equations of motion, solving the dynamics and then transforming back to the diabatic representation, it follows that the probability  $|c_2(t)|^2$  to find the qubit in diabatic state  $|2\rangle$  goes from zero to one as

$$|c_{2,\text{adiabatic}}(t)|^2 = \frac{1}{2} \left( 1 + \frac{Vt}{\sqrt{(Vt)^2 + 4f^2(t)}} \right). \quad (5)$$

The dependence for intermediate times on the interaction modulation  $f(t)$  is clearly seen. The four upper-left panels in figure 1 with  $\Omega = 0$  or  $0.5$  and  $g = 1$  or  $4$  are very well described by the adiabatic-following result (5).

### 3.2. Non-adiabatic regime

For phase  $\phi = 0$ , the Rabi coupling  $f(t)$  is zero at time  $t = \pi/2\Omega$  and the energy splitting becomes  $\pi V/2\Omega$ . This means that for a large driving frequency  $\Omega > \sqrt{V/\hbar}$ , the adiabaticity condition is violated. The data shown in the right columns of figure 1 indicate that in this regime the dynamics consists of two transitions at times  $\mp \hbar\Omega/V$ . If the time  $2\hbar\Omega/V$  between the individual transitions is sufficiently large, as specified below, the two transitions are essentially independent of each other. Then, it is possible to derive within a RWA an analytical expression for the final transition probability. The derivation is closely related to the transfer-matrix method employed in [36, 41].

With the new variables  $d_1(t) = \tilde{c}_1 \exp(i\hbar\Omega^2/4V)$  and  $d_2(t) = \tilde{c}_2 \exp(-i\hbar\Omega^2/4V)$ , one obtains from equation (2) the equations of motion

$$\dot{d}_1 = -i\frac{g}{2\hbar} [e^{iV(t+\hbar\Omega/V)^2/2\hbar} + e^{iV(t-\hbar\Omega/V)^2/2\hbar}] d_2, \quad (6)$$

$$\dot{d}_2 = -i\frac{g}{2\hbar} [e^{-iV(t+\hbar\Omega/V)^2/2\hbar} + e^{-iV(t-\hbar\Omega/V)^2/2\hbar}] d_1. \quad (7)$$

Like in equation (2), the phases on the right-hand side obey a quadratic time dependence. Thus, with the arguments provided after equation (3), we can conclude that each phase factor is relevant only at times at which the phase is stationary, i.e., the first term contributes only at time  $t_- = -\hbar\Omega/V$ , while the second term becomes relevant at time  $t_+ = \hbar\Omega/V$ . Thus, we keep at both times  $t_-$  and  $t_+$  only the respective resonant term while the ‘counter-rotating’ term is neglected. (In this case, two separate RWAs are needed corresponding to  $t_+$  and  $t_-$ .) Then, at times close to  $t_{\mp}$ , the equation of motion is of the same form as equation (2) and the dynamics is determined by the S-matrix (3) with  $g$  replaced by  $g/2$ , i.e.  $\mathbf{S}_{\mp} = \mathbf{S}_{g/2}$ . Consequently within the transfer-matrix approximation, the time evolution becomes

$$|\tilde{\psi}(t)\rangle = \begin{cases} |\psi(-\infty)\rangle & \text{for } t < -\hbar\Omega/V, \\ \mathbf{S}_{g/2} |\psi(-\infty)\rangle & \text{for } -\hbar\Omega/V < t < \hbar\Omega/V, \\ \mathbf{S}_{g/2}^2 |\psi(-\infty)\rangle & \text{for } t > \hbar\Omega/V. \end{cases} \quad (8)$$

With this expression, the probability to find the system at time  $t = \infty$  in state  $|2\rangle$  is readily evaluated as

$$P = |\langle 2 | \mathbf{S}_{g/2}^2 | 1 \rangle|^2 = 4 e^{-\pi g^2/2\hbar V} (1 - e^{-\pi g^2/2\hbar V}). \quad (9)$$

During the intermediate times  $-\hbar\Omega/V < t < \hbar\Omega/V$ , the occupation probability of level  $|2\rangle$  becomes

$$P_{\text{int}} = |\langle 2 | \mathbf{S}_{g/2} | 1 \rangle|^2 = 1 - \exp(-\pi g^2/2\hbar V). \quad (10)$$

Note that in these expressions, the exponent differs from the exponent in equation (4) by a factor  $1/4$ . Moreover,  $P$  in equation (9) no longer depends monotonously on the coupling strength as in the standard LZ problem, but rather assumes a maximum for  $\exp(-\pi g^2/2\hbar V) = \frac{1}{2}$ . Interestingly enough, the transfer-matrix results are independent of the Stokes phase  $\chi$  and the modulation frequency  $\Omega$ . The independence of the frequency is confirmed by figure 1, where the transfer-matrix results (red lines) nicely agree with the exact results (blue lines) for  $\Omega = 2, 10$  and  $40$ . Clearly, at long times, the probability  $|c_2|^2$  is a function of only the coupling strength  $g$ .

Below, we will compare more systematically the transition probabilities obtained from the transfer-matrix method with a numerically exact solution. But first we have to specify the conditions under which the time between two LZ transitions will be long enough for the transfer-matrix analysis to hold. It should be remembered that LZ transitions neither occur instantaneously nor take infinitely long [42]–[44]. The time  $2\hbar\Omega/V$  between the two-consecutive transitions should be larger than the duration of a single transition. It has been estimated that the standard LZ transition has a typical duration  $\tau_{\text{LZ}} \simeq \sqrt{\hbar/V}$ , when non-adiabatic transitions are

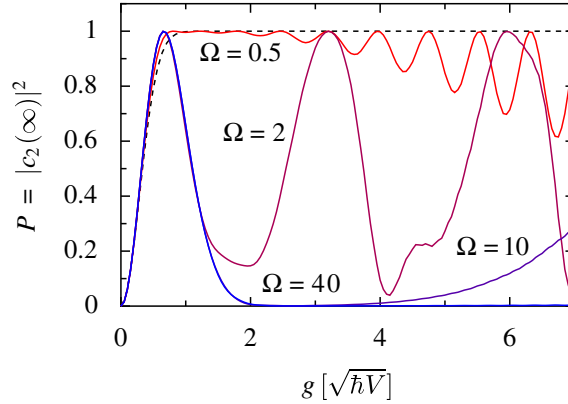


**Figure 3.** Final-transition probability  $P$  as a function of coupling  $g$ , for several values of the interaction-modulation frequency  $\Omega$ . The dashed line marks the standard LZ-transition probability (4) valid for  $\Omega = 0$ . The transfer-matrix result (9) coincides with the numerical result for  $\Omega = 40$ . (The numerical time integration was performed from times  $-500\sqrt{\hbar/V}$  to  $+500\sqrt{\hbar/V}$ ).

probable (i.e. for  $2g^2/(\hbar V) \ll 1$ ), while  $\tau_{\text{LZ}} \simeq 2g/V$  in the adiabatic limit  $2g^2/(\hbar V) \gg 1$  [42]. Correspondingly, reliable results of the transfer-matrix approach are to be expected if

$$\Omega \gtrsim \sqrt{V/(4\hbar)} \quad \text{for } g^2/(2\hbar V) \ll 1, \quad (11)$$

$$\Omega \gtrsim g/\hbar \quad \text{for } g^2/(2\hbar V) \gg 1. \quad (12)$$

These estimates are confirmed by the numerical solution of equation (2) as plotted in figure 3, which depicts the probability of finding the system in state  $|2\rangle$  at large times. The figure makes clear that for small coupling strengths  $g \ll \sqrt{\hbar V}$  the condition (11) is sufficient but not necessary, because equation (9) is seen to be accurate irrespective of the frequency. This is in accordance with the lower five panels in figure 1 and with fact that the standard LZ result (4) and the transfer-matrix expression (9) agree that  $P$  equals  $2\pi g^2/V$  to first order in  $g^2/V$ . On the other hand, we find significant deviations from the expression (9) once  $g$  becomes larger than  $\sqrt{\hbar V}$  and of the order  $\hbar\Omega$ . This is where the two LZ transitions start to ‘feel’ each other. For sufficiently large coupling, the transition probability even increases again and assumes further maxima with  $P = 1$ . It is nice that the argument can be turned around and that LZ times can be estimated with the help of the frequencies at which the exact and the transfer-matrix results start to deviate. In doing so, we indeed find (here and in section 4) that  $\tau_{\text{LZ}} \simeq 2g/V$  for  $2g^2/(\hbar V) \gg 1$ , in agreement with [42]. Thus, the present model provides an independent and simple method to determine LZ times.

#### 4. Exploring the crossover region

Our analysis has identified two different parameter regimes in which the analytical solution is confirmed by our numerical results. Firstly, there is the regime of slow driving in which  $\hbar\Omega$  denotes the smallest energy scale of the problem. Then, the time dependence of the coupling is not essential and the transition probabilities are the same as in the standard LZ problem. In the

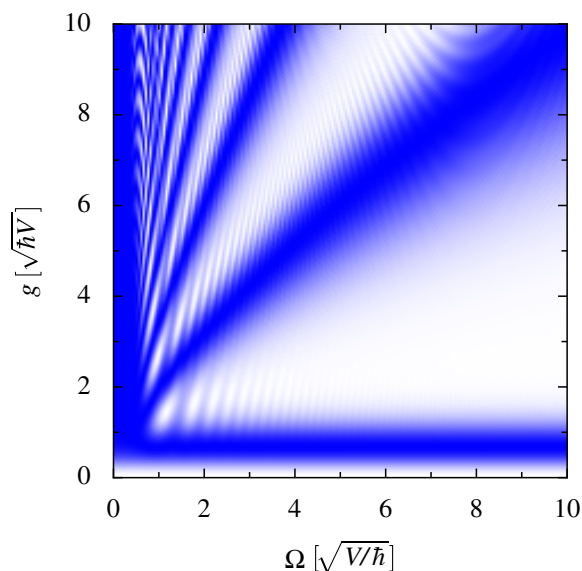


**Figure 4.** Final-transition probability  $P$  as a function of coupling strength  $g$  and frequency  $\Omega$ . Blue areas correspond to  $P = 1$ , white areas to  $P = 0$ .

second regime  $\hbar\Omega$  is the largest energy scale and the transfer-matrix results hold. In particular, we find  $P = 1$  for  $\pi g^2 = 2\hbar V \ln 2$ . In this section, we complement our analytical findings by numerical results for the intermediate-parameter regime.

Figure 4 shows the final transition probability, that is the occupation of state  $|2\rangle$  in the limit  $t \rightarrow \infty$ , as a function of both coupling strength  $g$  and frequency  $\Omega$ . The curves in figure 3 present vertical cuts through figure 4. The time interval for numerical integration was chosen the same as for figure 3. The vertical stripe with  $P = 1$  for  $\Omega \lesssim 0.5$  corresponds to the adiabatic regime. The horizontal blue stripe marks the maximum found within the transfer-matrix approach. The figure also confirms (i) that the location of the maximum has no significant frequency dependence and (ii) that  $P$  decays for a larger coupling  $g$  almost to zero, yielding the white region with  $P = 0$  above the horizontal blue band, in agreement with the transfer-matrix prediction (9). Increasing  $g$  further, we find that at  $g \approx \hbar\Omega$ , the transition probability again assumes values close to unity. This regime, including the sequence of maxima and minima that can be observed for even larger coupling, is beyond the range of validity of the transfer-matrix method. The fact that the transfer-matrix approach starts to break down along the diagonal  $g = \hbar\Omega$  in figure 4 neatly agrees with the estimate (12). With the reasoning given in section 3.2, we can infer from figure 4 that the estimate for the LZ time  $\tau_{\text{LZ}} \simeq 2g/V$  [42] holds at least in the broad-parameter regime  $1 < g^2/\hbar V < 100$ .

## 5. Phase dependence

When discussing the adiabatic energies of the Hamiltonian (1), we have already anticipated that the phase  $\phi$  might have some relevance which we explore in the following. For that purpose, we adapt the analytical approach of section 3.2 accordingly.

### 5.1. Transfer-matrix approach

Inserting again the definitions  $d_1 = \tilde{c}_1 \exp(i\hbar\Omega^2/4V)$  and  $d_2 = \tilde{c}_2 \exp(i\hbar\Omega^2/4V)$  into the equation of motion (2), we find

$$\dot{d}_1 = -i\frac{g}{2\hbar} [e^{iV(t+\hbar\Omega/V)^2/2\hbar+i\phi} + e^{iV(t-\hbar\Omega/V)^2/2\hbar-i\phi}] d_2, \quad (13)$$

$$\dot{d}_2 = -i\frac{g}{2\hbar} [e^{-iV(t+\hbar\Omega/V)^2/2\hbar-i\phi} + e^{-iV(t-\hbar\Omega/V)^2/2\hbar+i\phi}] d_1. \quad (14)$$

These equations differ from equation (2) merely by the phase  $\phi$  in the exponents. The goal is now to transform equations (13) and (14) such that they assume at times  $t_{\mp} = \mp \hbar\Omega/V$  the same form as equations (6) and (7). After such a transformation the transfer-matrix method could be used again. At time  $t_-$ , when only the first term in the equations of motion is relevant, an appropriate transformation reads

$$\mathbb{T} = \begin{pmatrix} e^{-i\phi/2} & 0 \\ 0 & e^{i\phi/2} \end{pmatrix}. \quad (15)$$

The corresponding transfer matrix  $\mathbb{S}_-$  follows from a transformation of  $\mathbb{S}_{g/2}$  with  $\mathbb{T}$  and reads  $\mathbb{S}_- = \mathbb{T}^{-1} \mathbb{S}_{g/2} \mathbb{T}$ . With the same reasoning, we find that at time  $t_+$  the required transformation is  $\mathbb{T}^{-1}$  and the transfer matrix is  $\mathbb{S}_+ = \mathbb{T} \mathbb{S}_{g/2} \mathbb{T}^{-1}$ . Consequently, the complete time evolution becomes  $|\tilde{\psi}(\infty)\rangle = \mathbb{S}_+ \mathbb{S}_- |\tilde{\psi}(-\infty)\rangle$ . This leads to the final transition probability

$$P = 4 e^{-\pi g^2/2V} (1 - e^{-2\pi g^2/2V}) \cos^2 \phi. \quad (16)$$

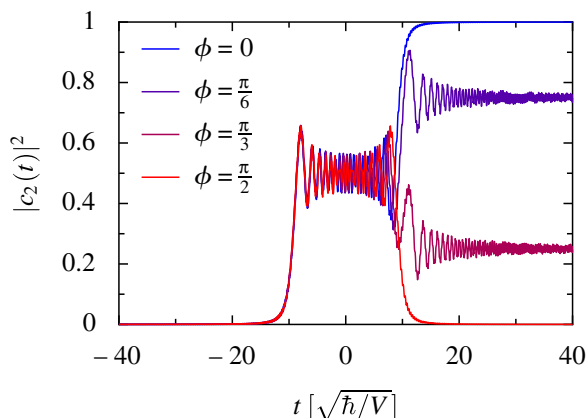
Clearly, the phase shift modifies the transition probability by a factor  $\cos^2 \phi$ . At intermediate times, the occupation is determined by  $\mathbb{S}_-$ . Interestingly enough, the absolute values of its matrix elements do not depend on  $\phi$  and, thus, we find at  $t = 0$  the same phase-independent transition probability  $P_{\text{int}}$  as in (10). Evidently, the phase dependence in (16) is caused by quantum interference between the two transition paths from  $|1\rangle$  to  $|2\rangle$ , which also explains the absence of any phase dependence after the first transition.

Figure 5 shows a comparison with the numerically computed time evolution. The long-time limits compare favourably with our prediction for the final state. As for the special case  $\phi = 0$ , the final occupation is independent of the frequency, provided that  $\Omega$  exceeds  $g/\hbar$  and  $\sqrt{V/\hbar}$ .

The strong-phase dependence in (16) may come as a surprise, since it is tempting to argue that for high frequencies, phase relations should be immaterial due to the many oscillations occurring during each LZ transition. However, figure 5 clearly demonstrates that such reasoning is incorrect.

### 5.2. Time-reversal anti-symmetry

The transition probability (16) obviously vanishes for  $\phi = \pi/2$ . This behaviour can already been obtained from symmetry arguments. For this phase, the Hamiltonian (1) is anti-symmetric under time reversion  $t \rightarrow -t$ , i.e.,  $H(t) = -H(-t)$ . Then the time evolution operators  $U(t, 0)$  and  $U(-t, 0)$  obey the same equation of motion. Moreover, they obviously are identical and equal



**Figure 5.** Transition probability as a function of time for  $g/\sqrt{\hbar V} = [2 \ln(2)/\pi]^{1/2} \approx 0.664$  and driving frequency  $\Omega = 10\sqrt{V/\hbar}$ . The transfer-matrix method predicts the intermediate population  $|c_2(0)|^2 = 0.5$  and the final-transition probabilities 1, 0.75, 0.25 and 0, respectively.

to  $\mathbf{1}$  at  $t = 0$ . The equalities  $U(\infty, 0) = U(-\infty, 0) = U^\dagger(0, -\infty)$  follow immediately, the last one from unitarity. Consequently, we find

$$U(\infty, -\infty) = U(\infty, 0)U(0, -\infty) = U^\dagger(0, -\infty)U(0, -\infty) = \mathbf{1}, \quad (17)$$

which implies that at long times, the system will evolve back to its initial state.

This ideal back-evolution relates our problem to the Loschmidt echo which has been employed for testing the sensitivity of a ‘chaotic’ quantum system on weak perturbations [45]. In the present case, the small parameter is  $\delta\phi = \phi - \pi/2$  which corresponds to the perturbation Hamiltonian  $\Sigma = -2g \cos(\Omega t) \sin(\delta\phi)\sigma_x$ . Note, however, that the present system does not exhibit any sensitive exponential dependence on the perturbation.

## 6. Discussion and summary

Our study of diabatic level crossing in a system subject to a time-dependent dipole force revealed two intriguing features. Firstly, the probability for non-adiabatic transitions is not simply a monotonous function of the coupling strength but exhibits several maxima and minima. In particular, it vanishes for zero coupling and equals unity if the relation  $g/\sqrt{\hbar V} = [2 \ln(2)/\pi]^{1/2} \approx 0.664$  is fulfilled. This is in contrast to the standard LZ problem where the extreme cases require a vanishing or an infinite interaction strength. Secondly, we found that the phase  $\phi$  of the dipole field has a significant influence on the transition probability which is proportional to  $\cos^2 \phi$ . The combination of both effects enables one to steer the system towards the one or the other final state. In turn, it is also possible to use the setup as a diagnostic tool for an unknown phase of a radiation field. The fact that the results of the transfer-matrix approach are only valid if the duration  $\tau_{LZ}$  of a single LZ transition is sufficiently small, provides a further application. Measuring the frequency at which the approximation breaks down, allows one to determine  $\tau_{LZ}$ .

*Practical requirements* for the applicability of our model are that the measurements (a) occur on a short enough time scale such that decoherence can be neglected, but (b) are slow enough such that the sweep rates of the driving fields are smaller than some values fixed by the experimental setup. *Theoretical requirements* for optimal observation of phase-dependent final-transition probabilities are (i) that there are two (almost) independent LZ transitions, separated by many periods of the interaction, in other words that the frequency  $\Omega$  should be much larger than  $\sqrt{V/\hbar}$ , and (ii) that  $g/\sqrt{\hbar V} \simeq 0.664$  (see section 5).

A straightforward physical realization of our set-up is naturally provided by spin- $\frac{1}{2}$  systems in time-dependent magnetic fields, with one magnetic field  $H_z(t)$  increasing linearly and a perpendicular field  $H_x(t) = H_x \cos(\Omega t + \phi)$  oscillating harmonically in time. Moreover, one could think of similar experiments with effective low-spin systems such as molecular nanomagnets [14, 46, 47]. Indeed, it would be interesting to repeat the recent resonant-photon absorption experiments on the effective spin- $\frac{1}{2}$  molecular complex  $V_{15}$  [47], this time with a non-negligible sweep rate of the longitudinal magnetic field  $H_z$ .

To be concrete, for a sweep rate of  $1 \text{ T s}^{-1}$ , a number of oscillations  $\Omega/\sqrt{V/\hbar} = 10$  as assumed in our figure 5, and for a parameter  $\gamma = g_z \mu_B / (4\pi\hbar) = 28.3 \text{ GHz T}^{-1}$  as measured for  $V_{15}$  in [47], one would need a very low frequency  $\Omega \simeq 5 \text{ MHz}$ , with corresponding temperature far below the mK regime. One can choose a higher frequency so that requirement (i) is satisfied even better, thereby increasing the time interval between the two LZ transitions. This time, however, is limited by requirement (a). For example, in the very recent LZ tunnelling measurements on molecular nanomagnets with the effective spin  $S = 9/2$  [48], the time between the LZ transitions is much too long for coherence effects in successive LZ transitions to be observable. Indeed, experiments on molecular nanomagnets are usually performed in the incoherent tunnelling regime, which is studied theoretically in [49, 50]. Still, we are convinced that our predicted phase-dependent effects can be observed in spin- $\frac{1}{2}$  systems such as the molecular complex  $V_{15}$ , by experiments at lower temperatures, lower frequencies, and higher sweep rates than those used in [48].

Another solid-state qubit to which our model might apply is a double-quantum dot [51]. This system is very well suited for LZ type experiments, because the energy level separation can be controlled simply by varying gate voltages. However, it might be a challenge to couple the levels via a transverse harmonic field. External fields usually couple to the qubit longitudinally [51], thereby bringing closer a realization of the harmonically perturbed LZ model [52], although energy changes might not be the only effects of the time-dependent external fields (see the discussion in section 2.4.1 of [40]). LZ processes in coupled quantum dots with time-varying tunnel couplings have been studied [53], but a difference with our model is that tunnel couplings do not change their signs. More promising realizations of our model are two-level systems found in double-quantum wells [38, 54], where the two levels can indeed be coupled by transverse electromagnetic fields (see also [55]).

A final possible realization is given by Rydberg atoms in the vicinity of a crossing of the highest Stark level in the  $n$ th manifold of the atom and the lowest Stark level of the  $(n + 1)$ th manifold [56, 57]. In this case, the energies are swept by the dc Stark effect and the interaction is driven by a harmonically varying microwave field. Then, the strong suppression of non-adiabatic transitions can be tested experimentally. Particularly promising in this respect would be variants of microwave ionization experiments of Rydberg atoms that are based on a mechanism of multiple LZ transitions to higher and higher Stark manifolds [57].

To summarize, we have studied LZ transitions in a two-level atom subject to a harmonically time-dependent, Rabi-like interaction. As a main difference to the standard LZ problem, we find that by tuning the coupling strength within a relatively small range, it is possible to continuously change the transition probability from zero to unity. This behaviour can be explained within a transfer-matrix approach, which provides reliable results provided that the driving frequency is sufficiently large. Moreover, this analytical approach allows one to determine the influence of the phase relation between the diabatic energy crossing and the dipole field. It revealed that the transition probability is proportional to  $\cos^2 \phi$  and therefore will vanish for  $\phi = \pi/2$ . The latter result was also shown by analysing the underlying time-reversal symmetry. The sensitive-phase dependence can be exploited both for steering the system towards a particular state and for measuring an *a priori* unknown phase relation.

## Acknowledgments

This work has been supported by the Freistaat Bayern via the quantum information initiative ‘Quantum Information Highway A8’ and by the Deutsche Forschungsgemeinschaft through SFB 631. KS and MW were supported by the Grant-in-Aid for Scientific Research of Priority Area from the Ministry of Education, Sciences, Sports, Culture and Technology of Japan (No 14077216).

## References

- [1] Nielsen MA and Chuang IL 2000 *Quantum Computation and Quantum Information* (Cambridge: Cambridge University Press)
- [2] Loss D and DiVincenzo D P 1998 *Phys. Rev. A* **57** 120
- [3] Landau L D 1932 *Phys. Z. Sowjetunion* **2** 46
- [4] Zener C 1932 *Proc. R. Soc. Ser. A* **137** 696
- [5] Stueckelberg E C G 1932 *Helv. Phys. Acta* **5** 369
- [6] Kayanuma Y 1984 *J. Phys. Soc. Japan* **53** 108
- [7] Grifoni M and Hänggi P 1998 *Phys. Rep.* **304** 229
- [8] Ankerhold J and Grabert H 2003 *Phys. Rev. Lett.* **91** 016803
- [9] Ithier G, Collin E, Joyez P, Vion D, Esteve D, Ankerhold J and Grabert H 2005 *Phys. Rev. Lett.* **94** 057004
- [10] Saito K and Kayanuma Y 2004 *Phys. Rev. B* **70** 201304(R)
- [11] Spreeuw R J C, Van Druten N J, Beiersbergen M W, Eliel E R and Woerdman J P 1990 *Phys. Rev. Lett.* **65** 3642
- [12] Shytov A V, Ivanov D A and Feigel'man M V 2003 *Eur. Phys. J. B* **36** 263
- [13] Izmailkov A *et al* 2004 *Europhys. Lett.* **65** 844
- [14] Miyashita S 1995 *J. Phys. Soc. Japan* **64** 3207
- [15] Wernsdorfer W and Sessoli R 1999 *Science* **284** 133
- [16] Farhi E, Goldstone J, Gutmann S and Sipser M 2000 Quantum computation by adiabatic evolution *Preprint* quant-ph/0001106
- [17] Steffen M, Van Dam W, Hogg T, Breyta G and Chuang I 2003 *Phys. Rev. Lett.* **90** 067903
- [18] Rabi I I 1937 *Phys. Rev.* **51** 652
- [19] Schwinger J 1937 *Phys. Rev.* **51** 648
- [20] Allen L and Eberly J H 1975 *Optical Resonance and Two-Level Atoms* (New York: Wiley)
- [21] Mandel L and Wolf E 1995 *Optical Coherence and Quantum Optics* (Cambridge: Cambridge University Press)
- [22] Bloch F and Siegert A 1940 *Phys. Rev.* **57** 522

- [23] Grossmann F, Dittrich T, Jung P and Hänggi P 1991 *Phys. Rev. Lett.* **67** 516
- [24] Grossmann F, Jung P, Dittrich T and Hänggi P 1991 *Z. Phys.* **84** 315
- [25] Grossmann F and Hänggi P 1992 *Europhys. Lett.* **18** 571
- [26] Kayanuma Y 1985 *J. Phys. Soc. Japan* **54** 2037
- [27] Nishino M, Saito K and Miyasjita S 2001 *Phys. Rev. B* **65** 014403
- [28] Pokrovsky V L and Sinitsyn N A 2003 *Phys. Rev. B* **67** 144303
- [29] Gefen Y, Ben-Jacob E and Caldeira A O 1987 *Phys. Rev. B* **36** 2770
- [30] Ao P and Rammer J 1991 *Phys. Rev. B* **43** 5397
- [31] Shimshony E and Gefen Y 1991 *Ann. Phys. NY* **210** 16
- [32] Akulin V M and Schleich W P 1992 *Phys. Rev. A* **46** 4110
- [33] Kayanuma Y and Nakayama H 1998 *Phys. Rev. B* **57** 13099
- [34] Shytov A V 2000 Dissipative Landau–Zener tunnelling at marginal coupling *Preprint cond-mat/0001012*
- [35] Saito K and Kayanuma Y 2002 *Phys. Rev. A* **65** 033407
- [36] Kayanuma Y 1994 *Phys. Rev. A* **50** 843
- [37] Garraway B M and Vitanov N V 1997 *Phys. Rev. A* **55** 4418
- [38] Platero G and Aguado R 2004 *Phys. Rep.* **395** 1
- [39] Kohler S, Lehmann J and Hänggi P 2005 *Phys. Rep.* **406** 379
- [40] Brandes T 2005 *Phys. Rep.* **408** 315
- [41] Kayanuma Y 1993 *Phys. Rev. B* **47** 9940
- [42] Mullen K, Ben-Jacob E, Gefen Y and Schuss Z 1989 *Phys. Rev. Lett.* **62** 2543
- [43] Vitanov N V and Garraway B M 1996 *Phys. Rev. A* **53** 4288
- [44] Vitanov N V 1999 *Phys. Rev. A* **59** 988
- [45] Jalabert R A and Pastawski H M 2001 *Phys. Rev. Lett.* **86** 2490
- [46] Sorace L, Wernsdorfer W, Thirion C, Barra A L, Pacchioni M, Mailly D and Barbara B 2003 *Phys. Rev. B* **68** 220407(R)
- [47] Wernsdorfer W, Müller A, Mailly D and Barbara B 2004 *Europhys. Lett.* **66** 861
- [48] Wernsdorfer W, Bhaduri S, Vinslava A and Christou G 2005 Landau–Zener tunneling in the presence of weak intermolecular interactions in a crystal of Mn<sub>4</sub> single-molecule magnets *Preprint cond-mat/0508608*
- [49] Thorwart M, Grifoni M and Hänggi P 2000 *Phys. Rev. Lett.* **85** 860
- [50] Leuenberger M N and Loss D 2000 *Phys. Rev. B* **61** 12200
- [51] Van der Wiel W G, De Franceschi S, Elzerman J M, Fujisawa T, Tarucha S and Kouwenhoven L P 2003 *Rev. Mod. Phys.* **75** 1
- [52] Kayanuma Y and Mizumoto Y 2000 *Phys. Rev. A* **62** 061401(R)
- [53] Renzoni F and Brandes T 2001 *Phys. Rev. B* **64** 245301
- [54] Holthaus M and Hone D 1993 *Phys. Rev. B* **47** 6499
- [55] Villas-Bôas J M, Zhang W, Ulloa S E, Rivera P H and Studart N 2002 *Phys. Rev. B* **66** 085325
- [56] Rubbmark J R, Kash M M, Littman M G and Kleppner D 1981 *Phys. Rev. A* **23** 3107
- [57] Pillet P, Van Linden van den Heuvell H B, Smith W W, Kachru R, Tran N H and Gallagher T F 1984 *Phys. Rev. A* **30** 280